Peer reviewed version

University of Bristol - Explore Bristol Research
General rights

A Novel Robust Adaptive Control Algorithm with Finite-Time Online Parameter Estimation of a humanoid robot arm.

M.N. Mahyuddin[a,1,], S.G. Khan[a,2], G. Herrmann[a,3]

[a]*Bristol Robotics Laboratory and Department of Mechanical Engineering, University of Bristol, University Walk, BS8 1TR, Bristol, United Kingdom.*

Abstract

A novel robust adaptive control algorithm is proposed and implemented in real-time on two degrees-of-freedom (DOF) of the humanoid Bristol-Elumotion-Robotic-Torso II (BERT II) arm in joint-space. In addition to having a significant robustness property for the tracking, the algorithm also features a sliding-mode term based adaptive law that captures directly the parameter estimation error. An auxiliary filtered regression vector and filtered computed torque is introduced. This allows the definition of another auxiliary matrix, a filtered regression matrix, which facilitates the introduction of a sliding mode term into the adaptation law. Parameter error convergence to zero can be guaranteed within finite-time with a Persistent-Excitation (PE) condition or Sufficient Richness condition for the demand. The proposed scheme also exhibits robustness both in the tracking and parameter estimation errors to any bounded additive disturbance. This theoretical result is then exemplified for the BERT II robot arm in simulation and for experiments.

Email addresses: `memnm@bristol.ac.uk` (M.N. Mahyuddin), `mesgk@bristol.ac.uk` (S.G. Khan), `g.herrmann@bristol.ac.uk` (G. Herrmann)

[1]Muhammad Nasiruddin Mahyuddin is currently doing a PhD in the Bristol Robotics Laboratory and the Department of Mechanical Engineering, University of Bristol. His PhD is sponsored by University Sains Malaysia and Ministry of Higher Education Malaysia.

[2]Said Ghani Khan is a post-doctorate holding a research assistant position at the Department of Mechanical Engineering, University of Bristol.

[3]Guido Herrmann is a Reader in Control and Dynamics at the Department of Mechanical Engineering, University of Bristol and a theme leader at the Bristol Robotics Laboratory.

1. Introduction

For several years, many researchers have been interested in the adaptive control of rigid robot manipulators. Due to the fact that, robot manipulators are inherently nonlinear, multi-input-multi-output (MIMO) with significant couplings between its link members, the task of capturing this vital information for control purposes can become challenging. This calls for the incorporation of adaptive methods whereby adaptive control is used to estimate parameters of the manipulator model recursively and use the estimates in the control scheme, e.g. [1, 2, 3, 4, 5]. Work in adaptive control of robot manipulators began with controlling a linear perturbed model with adaptive high gains [6, 7, 8, 9] followed by globally convergent adaptive control results as summarised in [10].

A turning point in adaptive robotic control research took place in the mid 1980s when linear parametrisation of the nonlinear robot dynamics was explicitly introduced [2]. A repertoire of adaptive control schemes for robot manipulators has been formulated of which three main classes of adaptive control can be classified; direct adaptive control [11, 12, 13], indirect adaptive control [14, 15] and composite adaptive control [2]. Work in [13] demonstrates computed-torque based adaptive control and proves its global convergence. What limits the practical applicability of such direct adaptive control is that the approach requires joint acceleration measurements and an inverse of the estimated inertia which is susceptible to noise. Moreover, reliance on the inversion of the estimated inertia is computationally expensive. Such restrictive assumptions as outlined in [13] can be resolved by methods introduced in [2, 16] and will be discussed briefly in our paper as part of the adaptive algorithm formulation framework.

Work on an indirect model based adaptive control of a humanoid manipulator arm is demonstrated in [17]. Most of the indirect and composite adaptive control approaches presented in [11, 12, 14] demonstrate that the tracking and prediction/estimation error can be utilised to extract parameter information. The objective is to guarantee convergence and performance, in particular, the tracking control of a robotic arm. Previous restrictive assumptions were resolved. Their approaches, with the condition of persistent excitation (PE) or under the assumption of a sufficiently rich demand, guarantee

the convergence to zero of both the tracking error and prediction error by the introduction of the bounded-gain-forgetting method and the cushioned-floor method. However, only exponential convergence of tracking and parameter error are theoretically proven in their proposed scheme [14, 2]. This motivates us to investigate further and propose to use a novel adaptive algorithm [18] that guarantees a finite-time convergence in particular for the parameter error convergence to zero for a practical robotic arm control problem.

In this paper, inspired by the work in [19] and extending our previous work in [18],[20] and [21], a novel robust adaptive algorithm is proposed for control of a robotic manipulator. This controller utilises the parameter estimation error in the adaptive control scheme through the incorporation of an auxiliary regression matrix and vector that reconstruct the parameters to be estimated. A sliding-mode like adaptation term is introduced for finite-time convergence of the estimated parameter to the true value. With the addition of sliding-mode terms in the tracking (in constrast to [21]) and in the parameter estimation algorithm, robustness is introduced both in the tracking as well as in the parameter estimation performance. The introduction of a disturbance into the analysis also requires a different approach, in contrast to [21], to the proof of stability to guarantee boundedness in particular for the auxiliary (filtered) regressor matrix. In contrast to [22] of mere σ-modification, a special leakage term is incorporated in our work, that captures the parameter estimation error and aids robustness. Moreover, inspired by [16], acceleration measurements are avoided in the regressor formulation by the virtue of torque filtering through the use of strictly proper monic stable filters. The use of torque filtering has several wide applications in robotics such as impedance control [23] (generating a generic unified error equation), parameter estimation [16] (to form a prediction error to be used in LS estimator), fault detection [24] (to form a prediction error) and others. However, the use of torque filtering in this paper is unique in a sense that the formulation of the filtered regressor avoids acceleration information and permits parameters to be estimated within finite time. As proven in [25], the filtered regressors, i.e. the filtered computed torque and dynamic regressors inherit the PE characteristics of the original signal. It can be also proven, that the PE condition can be fulfilled by proper selection of the demand trajectory signal that satisfies the PE condition or sufficient richness condition (SR).

This paper is divided into four sections. The first section, which is the problem formulation section, presents the dynamic model of the robot being

investigated. The second section which is the Adaptive Control Algorithm section discusses the main contribution of the paper, i.e. the formulation of the novel robust adaptive control algorithm for a robotic system. The third section discusses the experimental setup and results; it exemplifies the performance of the proposed algorithm by careful simulation and experimental setup. The last section concludes the findings.

2. Problem Formulation

The humanoid Bristol Elumotion Robotic Torso II (Bristol Elumotion Robotic Torso II is developed by Elumotion Ltd) or BERT II robotic arm is a highly nonlinear and coupled system. We assume the general structure of the robot dynamics is given by:

$$M(q)\ddot{q} + c(q, \dot{q}) + G(q) + T_d = \tau \tag{1}$$

where $q = q(t), \dot{q} = \dot{q}(t), \ddot{q} = \ddot{q}(t) \in \mathbb{R}^n$ are the robot arm joint position, velocity and acceleration vectors respectively; n is the number of degrees of freedom (DOF) of the robot, $\tau \in \mathbb{R}^n$, the input torque vector; $M(q) \in \mathbb{R}^{n \times n}$, $M(q) > 0$, is the inertia matrix, a function of the n joint positions q. T_d is an $n \times 1$ vector representing an additive bounded disturbance. The vector

$$c(q, \dot{q}) = V(q, \dot{q})\dot{q} = (I_n \otimes \dot{q}^T)C_v(q)\dot{q} \in \mathbb{R}^n \tag{2}$$

employs $C_v(q) = [C_1^T(q), \cdots, C_n^T(q)]^T \in \mathbb{R}^{nn \times n}$ which represents the Coriolis/centripetal torque, viscous and nonlinear damping. $G(q) \in \mathbb{R}^n$ is the torque vector due to gravity. Several essential properties for (1) facilitate the adaptive control system design:

Property 1. *Passive mapping from input τ to output $\dot{q}$ implies that $\dot{M}(q) - 2V(q, \dot{q})$ is a skew-symmetrical matrix [26],[16]:*

$$\xi^T \left(\dot{M}(q) - 2V(q, \dot{q}) \right) \xi = 0 \tag{3}$$

Property 2. *The left hand side of (1) can be linearly parameterised as such,*

$$M(q)\ddot{q} + c(q, \dot{q}) + G(q) = \phi(q, \dot{q}, \ddot{q})\Theta \tag{4}$$

where $\Theta \in \mathbb{R}^l$ is the system parameter vector containing l parameters to be estimated; $\phi(q, \dot{q}, \ddot{q}) \in \mathbb{R}^{n \times l}$ is the known dynamic regression matrix, a Lipschitz continuous function of $(q, \dot{q}, \ddot{q})$ [1].

Property 3. *It is assumed that the demand q_d is at least twice continuously differentiable with time t and q_d is sufficiently rich (SR) over a finite interval $[t, t + T]$ of the specific length $T > 0$ with respect to $\phi(q_d, \dot{q}_d)$, i.e. there exist at least l time instances $t_i, i = 1, 2, \ldots$ so that for $t_1, t_2, \ldots, t_l \in [t, t + T]$*

$$\Phi(q_d(\cdot)) = [(\phi(q_d(t_1)))^T, (\phi(q_d(t_2)))^T, \cdots, (\phi(q_d(t_l)))^T] \tag{5}$$

is of rank l and there is a finite constant $\delta > 0$ so that the following matrix inequality holds [25], [27],

$$\Phi^T(q_d(\cdot))\Phi(q_d(\cdot)) \geq \delta I, \delta > 0 \tag{6}$$

Remark 1. *Some further derivation implies from Property 3 that*

$$\int_t^{t+T} \phi^T(q_d(\nu), \dot{q}_d(\nu))\phi(q_d(\nu), \dot{q}_d(\nu))d(\nu) > \tilde{\delta} I \tag{7}$$

for some $\tilde{\delta} > 0$. Note that this property (7) implies Persistent Excitation (PE), once the tracking controller follows this trajectory. This is to be discussed later. ○

The regression matrix ϕ is given in Property 2. It has the acceleration as argument. Note that in our proposed adaptive control algorithm, the regression matrix is to be reformulated, eradicating the need for the joint acceleration unlike in [28]. This is inspired by [16] where similar approaches are used to avoid acceleration measurements.

3. Adaptive Control Algorithm

Define the auxiliary command vector as,

$$
\begin{align}
u &= \dot{q}_d - \Lambda e, \quad e = q_d - q \tag{8} \\
\dot{u} &= \ddot{q}_d - \Lambda \dot{e}, \quad \dot{e} = \dot{q}_d - \dot{q} \tag{9}
\end{align}
$$

with $e, \dot{e} \in \mathbb{R}^n$ denoting the error in tracking the desired joint position $q_d(t)$ and velocity $\dot{q}_d(t)$ respectively. $\Lambda = diag(\lambda_1, \lambda_2, \ldots, \lambda_n)$ is a positive diagonal matrix to be chosen in the design. A sliding-mode error can be written for each joint in a form of,

$$r_i = \dot{e}_i + \lambda_i e_i, \quad i = 1, \cdots, n, \quad r = [r_1, \ldots, r_n]^T \tag{10}$$

where λ_i is the sliding mode gain for each respective joint that defines the sliding manifold r_i. For control, the following input is proposed,

$$\tau = \hat{M}(q)\dot{u} + \hat{V}(q,\dot{q})u + \hat{G}(q) + K_{r_1}\frac{r}{\|r\|} + K_{r_2}r \qquad (11)$$

where K_{r_1} and K_{r_2} are scalar tracking gains. The matrices $\hat{M}(q)$ and $\hat{V}(q,\dot{q})$ are the estimates of the mass matrix $M(q)$ and the Coriolis, centrifugal matrix $V(q,\dot{q})$. The computed torque in (1) would yield,

$$M(q)\ddot{q} + V(q,\dot{q})\dot{q} + G(q) + T_d = \hat{M}(q)\dot{u} + \hat{V}(q,\dot{q})u + \hat{G}(q) + K_{r_1}\frac{r}{\|r\|} + K_{r_2}r \quad (12)$$

Subtracting $M(q)\dot{u} + V(q,\dot{q})u + G(q)$ on both sides of equation (12) implies,

$$\tilde{M}(q)\dot{u} + \tilde{V}(q,\dot{q})u + \tilde{G}(q) - K_{r_1}\frac{r}{\|r\|} - K_{r_2}r = M(q)(-\ddot{q}+\dot{u}) + V(q,\dot{q})(-\dot{q}+u) - T_d \tag{13}$$

where $\tilde{M}(q) = M(q) - \hat{M}(q)$, $\tilde{V}(q,\dot{q}) = V(q,\dot{q}) - \hat{V}(q,\dot{q})$ and $\tilde{G}(q) = G(q) - \hat{G}(q)$. Therefore, the closed-loop computed torque equation is:

$$\tilde{M}(q)\dot{u} + \tilde{V}(q,\dot{q})u + \tilde{G}(q) + T_d = \quad M(q)\dot{r} + V(q,\dot{q})r + K_{r_1}\frac{r}{\|r\|} + K_{r_2}r \tag{14}$$

$$\phi(q,\dot{q},u,\dot{u})\tilde{\Theta} + T_d = \quad M(q)\dot{r} + V(q,\dot{q})r + K_{r_1}\frac{r}{\|r\|} + K_{r_2}r \tag{15}$$

where $T_d = 0$ and $\phi(q,\dot{q},u,\dot{u}) \in \mathbb{R}^{n\times l}$ is the regressor from (2) but now with arguments u and $\dot{u}$ instead of $\ddot{q}$. Thus, the regressor forms a function of joint position q, velocity $\dot{q}$, and the command vectors $u, \dot{u}$. $\tilde{\Theta} = \Theta - \hat{\Theta} \in \mathbb{R}^l$ is the parameter estimation error. The next section provides some preliminary results for the adaptation algorithm in particular the regressor $\phi(q,\dot{q},\ddot{q})$ is investigated.

3.1. Auxiliary Torque Filters

In this section, an auxiliary filtered regression matrix and suitable filtered vectors for the adaptation algorithm will be formulated based on the torque measurement. By having the torque measurement filtered, acceleration measurements for the regressor $\phi(q,\dot{q},\ddot{q})$ can be avoided. Indeed, the regressor $\phi(q,\dot{q},\ddot{q})$ in (4) uses joint accelerations which generally is not practical. Hence, the equation (1) can be written as,

$$\tau = \dot{f} + h \tag{16}$$

6

The components of torque can be split and defined as,

$$\dot{f} = \frac{d}{dt}[M(q)\dot{q}] \tag{17}$$

$$h = -\dot{M}(q)\dot{q} + V_m(q,\dot{q})\dot{q} + G(q) = h_1 + h_2 \tag{18}$$

where $h_1 = -\dot{M}(q)\dot{q}$ and $h_2 = V_m(q,\dot{q})\dot{q} + G(q)$. By virtue of the linearity-in-the-parameter assumption, the split terms can be parameterised as such,

$$f = M(q)\dot{q} = \varphi_{m1}(q,\dot{q})\Theta \tag{19}$$

$$h_1 = -\dot{M}(q)\dot{q} = \varphi_{m2}(q,\dot{q})\Theta \tag{20}$$

$$h_2 = V_m(q,\dot{q})\dot{q} + G(q) = \varphi_{vg}(q,\dot{q})\Theta \tag{21}$$

Filtering the terms $\varphi_{m1}, \varphi_{m2}$ and φ_{vg} above provides:

$$\kappa\dot{\varphi}_{m1f}(q,\dot{q}) + \varphi_{m1f}(q,\dot{q}) = \varphi_{m1}(q,\dot{q}), \quad \phi_{m1_f}|_{t=0} = 0 \tag{22}$$

$$\kappa\dot{\varphi}_{m2f}(q,\dot{q}) + \varphi_{m2f}(q,\dot{q}) = \varphi_{m2}(q,\dot{q}), \quad \phi_{m2_f}|_{t=0} = 0 \tag{23}$$

$$\kappa\dot{\varphi}_{vgf}(q,\dot{q}) + \varphi_{vgf}(q,\dot{q}) = \varphi_{vg}(q,\dot{q}), \quad \phi_{vg_f}|_{t=0} = 0 \tag{24}$$

To aid the analysis in the case of a disturbance, the introduced additive bounded disturbance T_d is also assumed to be filtered,

$$\kappa\dot{T}_{df} + T_{df} = T_d, \quad T_{df}|_{t=0} = 0 \tag{25}$$

Eventually, the torque will be then filtered,

$$\kappa\dot{\tau}_f + \tau_f = \tau, \quad \tau_f|_{t=0} = 0 \tag{26}$$

to yield the filtered computed torque equation of the form,

$$\tau_f = F * \tau = \frac{1}{\kappa}e^{-t/\kappa} * [\dot{\varphi}_{m1}(q,\dot{q}) + \varphi_{m2}(q,\dot{q}) + \varphi_{vg}(q,\dot{q})]\Theta \tag{27}$$
$$+ \frac{1}{\kappa}e^{-t/\kappa} * T_d$$

where $*$ is the convolution operator F is the impulse response of a linear stable, strictly proper filter with κ denoting the time constant of the filter

for $\{\dot{\varphi}_{m1}(\cdot), \varphi_{m2}(\cdot), \varphi_{vg}(\cdot)\} \in \mathbb{R}^{n \times l}, \Theta \in \mathbb{R}^l$. The filtered computed-torque equation can be rewritten as,

$$\left[\frac{\varphi_{m1}(q, \dot{q}) - \varphi_{m1f}(q, \dot{q})}{\kappa} + \varphi_{m2f}(q, \dot{q}) + \varphi_{vgf}(q, \dot{q}) \right] \Theta + T_{df} = \tau_f \qquad (28)$$

$$\phi_f(q, \dot{q})\Theta + T_{df} = \tau_f$$

where $\phi_f(q, \dot{q}) \in \mathbb{R}^{n \times l}, \Theta \in \mathbb{R}^l$. By comparison to (1), the filtered system equation of (28) clearly avoids the acceleration measurements which are sometimes practically unavailable. Note that $\phi(q, \dot{q}, \ddot{q})$ is the unfiltered regressor for $\phi_f(q, \dot{q})$.

3.2. Auxiliary Integrated Regressors

The filtered torque formulation is now considered for an auxiliary regressor used for the adaptation algorithm. Define a filtered regressor matrix $W(t)$ and vector $N(t)$ as,

$$\dot{W}(t) = -k_{FF}W(t) + k_{FF}\phi_f^T(q, \dot{q})\phi_f(q, \dot{q}), \quad W(0) = kI, \qquad (29)$$

$$\dot{N}(t) = -k_{FF}N(t) + k_{FF}\phi_f^T(q, \dot{q})\tau_f, \quad N(0) = 0 \qquad (30)$$

where, $k_{FF} \in \mathbb{R}^+$, can be interpreted as a forgetting factor. The initial condition of $N(t)$ is $N(0) = 0$ whereas the initial condition of $W(t)$, i.e. $W(0)$ is set to kI where $k > 0$ is some constant and $I \in \mathbb{R}^{l \times l}$ is the identity matrix. Practically, k should be chosen small. Note that (30) is equivalent to:

$$\dot{N}(t) = -k_{FF}N(t) + k_{FF}\phi_f^T(q, \dot{q}) \left[\phi_f(q, \dot{q})\Theta + T_{df} \right], \qquad (31)$$

Consequently, we can find the solution to (29) and (30),

$$\begin{aligned} W(t) &= \int_0^t e^{-k_{FF}(t-r)}k_{FF}\phi_f^T(r)\phi_f(r)dr + e^{-k_{FF}t}kI \\ N(t) &= \int_0^t e^{-k_{FF}(t-r)}k_{FF}\phi_f^T(r)\tau_f dr \end{aligned} \qquad (32)$$

The solution to the auxiliary regressor vector $N(t)$ in (32) can be also expressed as,

$$N(t) = W(t)\Theta + T_{dN} - e^{-k_{FF}t}k\Theta, \qquad (33)$$

where $T_{dN} = \int_0^t e^{-k_{FF}(t-r)}k_{FF}\phi_f^T(r)T_{df}(r)dr$.

Referring to the solution of $\dot{W}(t)$ in (32), it is apparent that $W(t) \geq kIe^{-k_{FF}t}$ for $k > 0$. This bound will be exploited in the Lyapunov analysis section later.

8

3.3. Adaptive Control Law

The control law of (11), can be rewritten as,

$$\tau = \phi(q, \dot{q}, u, \dot{u})\hat{\Theta} + K_{r_1}\frac{r}{\|r\|} + K_{r_2}r \tag{34}$$

where $\hat{\Theta}$ is the estimate of the parameter vector Θ. An adaptive update law $\dot{\hat{\Theta}}$ is proposed, for $\hat{\Theta}$:

$$\dot{\hat{\Theta}} = \Gamma\phi^T(q, \dot{q}, u, \dot{u})r - \Gamma R. \tag{35}$$

In (35), Γ is a positive definite and diagonal design matrix:

$$\Gamma = diag(\gamma_1, \cdots, \gamma_l). \tag{36}$$

The term $R(t)$ contains a sliding mode type term to ensure fast parameter convergence whereby parameter estimates are constructed from the auxiliary regressor matrix $W(t)$ and vector $N(t)$,

$$R(t) = \omega_1\frac{W(t)\hat{\Theta} - N(t)}{\left\|W(t)\hat{\Theta} - N(t)\right\|} + \omega_2(W(t)\hat{\Theta} - N(t)) \tag{37}$$

where ω_1 and ω_2 are positive scalars which are to be chosen large enough to achieve robust stability. It will be proven that the parameter error vector, $\tilde{\Theta}$, converges to zero in finite time in case of $T_d = 0$. The following theorem summarizes the main result:

Theorem 1. *Given the control in (34) and the adaptation law in (35) and a suitably chosen bounded twice continuously differentiable, sufficiently rich (SR) demand q_d in (3), we can achieve*

1. *The trajectories, $q(t)$, converge to the demand q_d in a semiglobal sense, i.e. there exist a sliding mode gain matrix, Λ and gains $K_{r_1}, K_{r_2}, \omega_1, \omega_2 \in \mathbb{R}^+$ large enough so that exponential convergence is guaranteed for bounded disturbance, T_d.*
2. *The estimation error $\tilde{\Theta}$ converges to an ultimately bounded set in case of a bounded disturbance, T_d.*
3. *The estimate $\hat{\Theta}$ converges to their true values, in case of $T_d = 0$, within finite-time.*

$$\diamond$$

Proof . A suitable Lyapunov function is,

$$
\begin{aligned}
\mathcal{V}(t) &= \mathcal{V}_r + \mathcal{V}_\Theta \\
&= \frac{1}{2} r^T M(q) r + \frac{1}{2} \tilde{N}^T W^{-1} \Gamma^{-1} W^{-1} \tilde{N}
\end{aligned}
\tag{38}
$$

where,

$$
\begin{aligned}
\tilde{N}(t) &= N(t) - W(t)\hat{\Theta} = W(t)\Theta + T_{dN} - W(t)\hat{\Theta} - e^{-k_{FF}t} kI\Theta \quad (39) \\
&= W(t)\tilde{\Theta} + T_{dN} - e^{-k_{FF}t} kI\Theta
\end{aligned}
$$

This Lyapunov function contrasts to [21] in particular the second term, as it allows for analysis of a bounded disturbance. Note that,

$$
W(t) \geq e^{-k_{FF}t} kI
\tag{40}
$$

and

$$
\bar{\sigma}(W^{-1}(t)) \leq \frac{1}{k} e^{k_{FF}t}
\tag{41}
$$

where $\bar{\sigma}(\cdot)$ denotes the largest singular value of a matrix. Thus, the inverse of $W(t)$ exists at time, $t > 0$. Differentiating the Lyapunov function with respect to time yields,

$$
\dot{\mathcal{V}}(t) = r^T M(q)\dot{r} + \frac{1}{2} r^T \dot{M}(q) r + \tilde{N}^T W^{-1} \Gamma^{-1} \frac{\partial}{\partial t} \left[W^{-1} \tilde{N} \right]
\tag{42}
$$

as $r = \dot{e} + \Lambda e$ and $\dot{r} = \ddot{e} + \Lambda \dot{e}$. Computing the derivative of $W^{-1}\tilde{N} = \tilde{\Theta} + W^{-1} T_{dN} - W^{-1} e^{-k_{FF}t} kI\Theta$ provides

$$
\begin{aligned}
\frac{\partial}{\partial t} \left[W^{-1} \tilde{N} \right] &= \dot{\tilde{\Theta}} + W^{-1} \dot{W} W^{-1} \left[T_{dN} - e^{-k_{FF}t} kI\Theta \right] \\
&\quad + W^{-1} \left[\dot{T}_{dN} + k_{FF} e^{-k_{FF}t} kI\Theta \right] \\
&= \dot{\tilde{\Theta}} + \xi
\end{aligned}
\tag{43}
$$
$$
\tag{44}
$$

where $\xi = W^{-1} \dot{W} W^{-1} \left[T_{dN} - e^{-k_{FF}t} kI\Theta \right] + W^{-1} \left[\dot{T}_{dN} + k_{FF} e^{-k_{FF}t} kI\Theta \right]$. Substituting (14) and (44) into (42) produces,

$$
\begin{aligned}
\dot{\mathcal{V}}(t) &= r^T \phi(q, \dot{q}, u, \dot{u})\tilde{\Theta} - r^T V(q, \dot{q}) r - r^T K_{r_1} \frac{r}{\|r\|} - r^T K_{r_2} r \quad (45) \\
&\quad + \frac{1}{2} r^T \dot{M}(q) r + \tilde{N}^T W^{-1} \Gamma^{-1} \left[\dot{\tilde{\Theta}} + \xi \right]
\end{aligned}
$$

10

Applying the skew-symmetric property, (1), yields,

$$\dot{\mathcal{V}}(t) = r^T \phi(q, \dot{q}, u, \dot{u})\tilde{\Theta} + \tilde{N}^T W^{-1}\Gamma^{-1}\left[\dot{\tilde{\Theta}} + \xi\right] - r^T K_{r_1}\frac{r}{\|r\|} - r^T K_{r_2}r. \quad (46)$$

Adopting the proposed novel adaptive law in (35), $\dot{\tilde{\Theta}} = -\dot{\hat{\Theta}} = -\Gamma\phi^T(q, \dot{q}, u, \dot{u})r + \Gamma R$ into (46) yields,

$$\begin{aligned}
\dot{\mathcal{V}} &= -r^T K_{r_1}\frac{r}{\|r\|} - r^T K_{r_2}r + r^T \phi(q, \dot{q}, u, \dot{u})\tilde{\Theta} \\
&\quad + \tilde{N}^T W^{-1}\Gamma^{-1}\left[-\Gamma\phi^T(q, \dot{q}, u, \dot{u})r + \Gamma R + \xi\right] \\
&= -r^T K_{r_1}\frac{r}{\|r\|} - r^T K_{r_2}r - W^{-1}T_{dN}\phi(q, \dot{q}, u, \dot{u})r \\
&\quad + W^{-1}e^{-k_{FF}t}kI\phi(q, \dot{q}, u, \dot{u})r + \tilde{N}^T W^{-1}[R + \Gamma^{-1}\xi]
\end{aligned} \quad (47)$$

Replacing $R(t)$ via (37), it follows from (39),

$$\begin{aligned}
\dot{\mathcal{V}} &= -r^T K_{r_1}\frac{r}{\|r\|} - r^T K_{r_2}r - W^{-1}T_{dN}\phi(q, \dot{q}, u, \dot{u})r \\
&\quad + W^{-1}e^{-k_{FF}t}kI\phi(q, \dot{q}, u, \dot{u})r + \omega_1\tilde{N}^T W^{-1}\frac{W\hat{\Theta} - N}{\|W\hat{\Theta} - N\|} \\
&\quad + \omega_2\tilde{N}^T W^{-1}(W\hat{\Theta} - N) + \tilde{N}^T W^{-1}\Gamma^{-1}\xi \\
&\leq -\|r\|K_{r_1} - \|r\|^2 K_{r_2} + \bar{\sigma}(W^{-1})\|T_{dN}\|\|\phi\|\|r\| \\
&\quad + ke^{-k_{FF}t}\bar{\sigma}(W^{-1})\|\phi\|\|r\| - \tilde{N}\left[\omega_1\underline{\sigma}(W^{-1}) - \bar{\sigma}(W^{-1})\|\Gamma^{-1}\|\|\xi\|\right] \\
&\quad - \omega_2\underline{\sigma}(W^{-1})\|\tilde{N}\|^2 \\
&\leq -\|r\|\left[K_{r_1} - \bar{\sigma}(W^{-1})\|T_{dN}\|\|\phi\| - ke^{-k_{FF}t}\|\bar{\sigma}(W^{-1})\phi\|\right] \\
&\quad - \|\tilde{N}\|\left[\omega_1\underline{\sigma}(W^{-1}) - \bar{\sigma}(W^{-1})\|\Gamma^{-1}\|\|\xi\|\right] \\
&\quad - \|r\|^2 K_{r_2} - \omega_2\underline{\sigma}(W^{-1})\|\tilde{N}\|^2
\end{aligned}$$

$$(48)$$
$$(49)$$
$$(50)$$

The proof is now continued in two steps: The first will show that finite-time convergence of r to zero is achieved. This will result in persistent excitation of the plant via a sufficiently rich demand, q_d, within a given time interval $[0, T]$. From the definition of r (37), it is evident that q converges to q_d in an exponential sense once $r = 0$. The second step shows that $W^{-1}(t)$ and $W(t)$ remains always bounded in terms of its largest singular values. This guarantees item 1 and 2 of Theorem 1. Item 3 then easily follows.

In step 1, we may consider first a compact set $\mathcal{C}$ in $(q, \dot{q}, (W^{-1}\tilde{N}))$ which is chosen to be large enough to contain the initial values of $q(t = 0), \dot{q}(t = 0)$ and $(W^{-1}\tilde{N})(t = 0)$. From (48) and definition (10), it easily follows that q,

$\dot{q}$ and $W^{-1}\tilde{N}$ will remain within $\mathcal{C}$ at least for finite-time T. Moreover, note that for $t \in [0, T], \bar{\sigma}(W^{-1}) < \frac{1}{k}e^{k_{FF}T}$ from (40). It is now possible to find a finite value $K_{r_{1a}}$ for $t \in [0, T]$ which satisfies;

$$K_{r_{1a}} > \frac{1}{k}e^{k_{FF}T}\|T_{dN}\|\|\phi\| + e^{k_{FF}T}\|\phi\| \tag{51}$$

Equally, there must be also a finite value ω_{1a} for $t \in [0, T]$ so that;

$$\omega_{1a} > k^{-1}e^{k_{FF}T}\bar{\sigma}(W)\|\Gamma^{-1}\|\|\xi\| \tag{52}$$

We may now define,

$$\omega_1 = \omega_{1a} + \omega_{1b}, \quad \omega_{1b}, \omega_{1a} > 0, \tag{53a}$$

$$K_{r_1} = K_{r_{1a}} + K_{r_{1b}}, \quad K_{r_{1a}}, K_{r_{1b}} > 0, \tag{53b}$$

Then, it follows from (48) for $t \in [0, T]$,

$$\dot{\mathcal{V}} \leq -\|r\|K_{r_{1b}} - \|\tilde{N}\|\omega_{1b}\underline{\sigma}(W^{-1}) \tag{54}$$

$$-\|r\|^2 K_{r_2} - \omega_2\underline{\sigma}(W^{-1})\|\tilde{N}\|^2 \tag{55}$$

This implies,

$$\dot{\mathcal{V}} \leq -\alpha\sqrt{\mathcal{V}_r}K_{r_{1b}} - \gamma\sqrt{\mathcal{V}_\Theta}\omega_{1b} \tag{56}$$

$$-\|r\|^2 K_{r_2} - \omega_2\underline{\sigma}(W^{-1})\|\tilde{N}\|^2 \tag{57}$$

where $\alpha = \frac{\sqrt{2}}{\bar{\sigma}(M(q))^{\frac{1}{2}}}$ and $\gamma = \frac{\sqrt{2}\underline{\sigma}(W^{-1})}{\bar{\sigma}(W^{-1})\|\Gamma^{-1}\|^{\frac{1}{2}}}$.

Considering that $(q, \dot{q}, (W^{-1}\tilde{N})) \in \mathcal{C}$ for $t \in [0, T]$, it follows that $\|\phi\|, \|\phi_f\|$ (28), $\bar{\sigma}(W)$(32) remain bounded within the time interval $[0, T]$. Note that ϕ is a Lipschitz continuous function of $q, \dot{q}, \dot{q}_d, \ddot{q}_d$. This also implies that $\underline{\sigma}(W^{-1})$ is strictly bounded from below by a positive constant for $t \in [0, T]$. Thus, $K_{r_{1b}}$ and ω_{1b} can be chosen large enough so that the Lyapunov function $\mathcal{V}(t)$ (38) converges to 0 within the finite interval $[0, \frac{T}{4}]$ (see for instance [29] for finite-time convergence). Moreover, it is possible to choose the positive elements of the diagonal matrix, Λ (8) and scalar, λ, large enough so that for $t \geq \frac{T}{2}$ for some arbitrary, small constants, $\delta_a, \delta_b, \delta_c$ and $\epsilon > 0$, the following inequalities hold,

$$\|q(t) - q_d(t)\| \leq \delta_a, \quad \|\dot{q}(t) - \dot{q}_d(t)\| \leq \delta_b, \quad \|\ddot{q}(t) - \ddot{q}_d(t)\| \leq \delta_c \tag{58}$$

$$\|\phi(q,\dot{q},\ddot{q}) - \phi(q_d,\dot{q}_d,\ddot{q}_d)\| \leq \varepsilon \qquad (59)$$

Since the reference trajectory q_d is bounded, there exists a constant $\eta > 0$ for small enough $k > 0$ such that

$$\int_t^{t+T_\Delta} \phi^T(q(\nu),\dot{q}(\nu),\ddot{q}(\nu))\phi(q(\nu),\dot{q}(\nu)\ddot{q}(\nu))d\nu > \eta I \qquad (60)$$

holds for all $t \geq \frac{T}{2}, T_\Delta < \frac{T}{4}$ and for suitable reference q_d. Now, knowing that the auxiliary regressor matrix $W(t)$ in (29) is constructed by virtue of a filtered regressor $\phi_f(q,\dot{q})$ whereby an impulse response stable filter $F(t) = \frac{1}{\kappa}e^{-t/\kappa}$ is used, one can assure for small $\kappa > 0$ that there is $\tilde{\eta}$ for $t > \frac{3T}{4}$;

$$\int_t^{t+T_\Delta} \phi_f^T(q(\nu),\dot{q}(\nu))\phi_f(q(\nu),\dot{q}(\nu))d\nu > \tilde{\eta}I \qquad (61)$$

The proof for such inheritance of the PE characteristic of a filtered signal can be found in [25]. This also implies that, $W(t) > \varrho I$ where $\varrho > 0$ is not a function of time t in contrast to (40). Moreover, $\bar{\sigma}(W(t))$ remains bounded due to the boundedness of $q,\dot{q},\dot{q}_d,\ddot{q}_d$. Thus, a large enough choice for ω_{1a} and $K_{r_{1a}}$ will guarantee,

$$K_{r_{1a}} > \max(\frac{1}{k}e^{k_{FF}T}\|T_{dN}\|\|\phi\| + e^{k_{FF}T}\|\phi\|, \qquad (62a)$$

$$\bar{\sigma}(W^{-1})\|T_{dN}\|\|\phi\| + ke^{-k_{FF}t}\bar{\sigma}(W^{-1})\|\phi\|) \qquad (62b)$$

$$\omega_{1a} > \max\left(\frac{\bar{\sigma}(W^{-1})}{\underline{\sigma}(W^{-1})}\|\Gamma^{-1}\|\|\xi\|, \quad k^{-1}e^{k_{FF}T}\bar{\sigma}(W)\|\Gamma^{-1}\|\|\xi\|\right) \qquad (62c)$$

similar to (51) and (52). This retains equation (62) valid and guarantees that $W(t)$ is invertible all time. Hence, it follows that the error $\tilde{N}(t)$ converges to 0 in finite time. Thus, $\tilde{\Theta}$ remains bounded, where the bound is determined by the magnitude of the disturbance, T_d, i.e. by ξ. Clearly for $\xi = 0$, $T_{d_N} = 0$ and $\tilde{\Theta} \to 0$ (see (39)) in finite time. ∎

Remark 2. *The contribution of this paper can be exemplified in contrast to other existing adaptive laws in the function $R(t)(37)$ associated with $\tilde{\Theta}$. Thus, the actual parameter error is the driver of the adaptation algorithm which permits finite-time convergence.*

In contrast, the other standard adaptive laws, such as the gradient-based and the least-square-based algorithm, are driven by the control error as outlined below:-

Gradient-based adaptive law [27][30][26][31]: *This is accomplished by having Θ updated by means of steepest-descent method, i.e., the update law is written as $\dot{\hat{\Theta}} = \Gamma\phi^T(q, \dot{q}, u, \dot{u})r$ with $R = 0$. The adaptation is driven by the control error r and the adaptation gain Γ is fixed.*

LS-based adaptive law [27][30][26][31]: *This is accomplished similar to the gradient-based approach but with the adaptation gain Γ being updated by the following $\dot{\Gamma} = \beta\Gamma - \Gamma\phi\phi^T\Gamma, \quad \Gamma(0) = \Gamma_0 = Q_0^{-1}$, where β is a design parameter, a forgetting factor for Γ, i.e., discounting past data and a penalty on the initial estimate $\hat{\Theta}_0$. $Q_0 = Q_0^T > 0$ is the inverse of the initial value of Γ_0. The convergence of the LS-based algorithm can be shown (as proven in [27] [25] [26]) to be exponential in comparison to the proposed novel algorithm which provides finite-time convergence.*

○

4. Experimental setup and Results

The implementation environment of the proposed novel robust adaptive control on BERT-II humanoid system is shown in Figure 1. The proposed adaptive control algorithm was coded in Simulink blocks by a PC/notebook and subsequently compiled into C code by RT-workshop and dSPACE software. The compiled C code is then downloaded into a dSPACE 1006 embedded system. The dSPACE system communicates at 1 kHz with the humanoid BERT II robot arm system via a controller area network (CAN) communication bus. ControlDesk, a dSPACE software, is used as an interface to monitor the signals sent across the CAN bus from the EPOS BLDC driver unit to the dSPACE embedded system and to modify vital controller parameters. This software allows data to be recorded to be analysed further using Matlab.
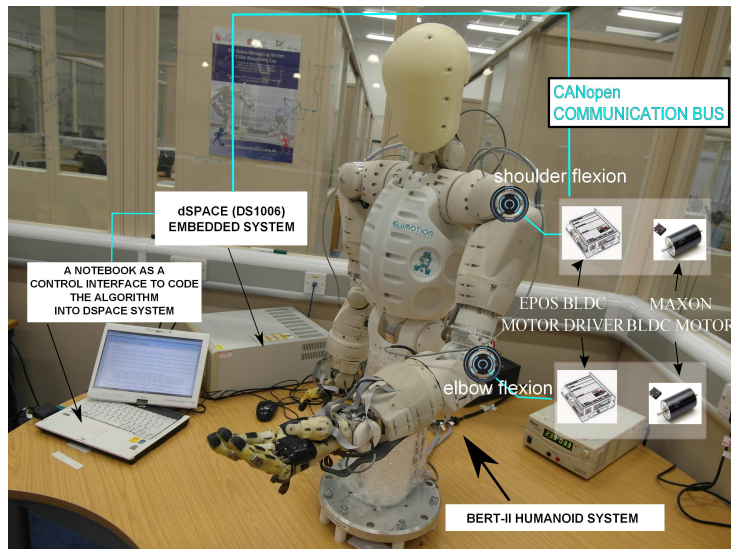
Figure 1: Bristol Elumotion Robot Torso II (BERT II) robotic arm system connected to the dSPACE. CANopen communication is established between dSPACE and the robot's actuator system.

The 7-degrees of freedom BERT II robot arm is equipped with MAXON high precision Brushless DC motors (BLDC) at each joint as actuators. Each motor is driven by an EPOS BLDC motor driver unit and the angular position of the motor is read by means of an incremental encoder (512cpr). The EPOS motor drivers at each joint are in fact connected to the dSPACE system by the CAN communication bus. The control signals sent via this CAN bus, are managed by a CANopen communication protocol using a periodic synchronisation signal. This allows a deterministic communication to be established in the CAN network without polling. In this experiment, 2 joints of the BERT II robot arm, the joints corresponding to shoulder flexion and elbow flexion motion, are to be controlled. The other joints of the arm such as shoulder abduction, humeral rotation, wrist pronation and other wrist related motion are kept in a fixed and straight position (by means of local PD controller regulation). Through these intended constraints, we are able to assume a two-link planar robot system as depicted in Figure 2. A cylindrical body mechanical structure throughout the BERT II's arm flexion and abduction with uniform mass distribution for the estimated parameters 2 is assumed. The mass of each robot link, the *upper arm* M_1 and the *forearm* M_2, are the elements of the mass matrix to be estimated, i.e. the estimated

parameter vector, $\hat{\Theta} = [\hat{M}_1, \hat{M}_2]^T$. The actual values of the approximated model of the BERT II arm is shown in Table 1.
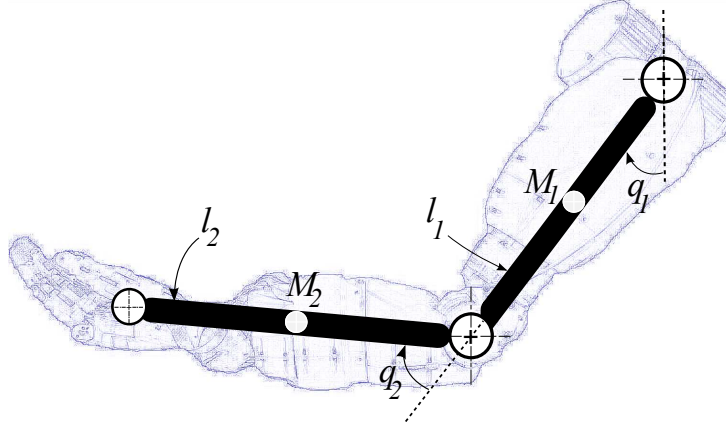

Figure 2: BERT II left arm can be modeled as two planar link system, using $M = M(q, \dot{q}, M_1, M_2)$

Table 1: The approximate model parameters of the BERT II arm

Description	Link 1	Link 2
Mass (kg)	2.35	3
Link Length (m)	0.2735	0.44
Radius of approximate cylindrical body (m)	0.05	0.05

4.1. Parameter Choice

Table 2 shows all the tuning parameters of the proposed novel algorithm used in the simulation and experiment. The parameter estimation adaptive weights Γ are selectively chosen to increase the sensitivity of the algorithm to the sliding error dynamics. Increasing Γ will definitely contribute to the increase of the finite-time convergence rate γ, associated with $\sqrt{V}_\Theta$ (see our analysis in the preceding section, equation (56)). However, the increase in Γ will make the estimation algorithm oversensitive to the sliding error dynamics which we want to avoid especially in the practical robotic system. The forgetting factor k_{FF} is carefully selected so as to ensure that the inverse of $W(t)$ in (32) exists. A large forgetting factor k_{FF} (associated with regressor matrix $W(t)$ and regressor vector $N(t)$) is desirable to allow for faster

convergence of the parameter estimation error to zero. A reasonably large value of k_{FF} also prevents the regressor matrix from growing unboundedly, compromising the need for conserving the immediate past horizon data (for better learning) and at the same time, ensuring faster parameter convergence. However, the value of k_{FF} cannot be made too large to permit $W(t)$ to be nonsingular. Knowing this importance, the filter constant, κ should be carefully selected so that the auxiliary filters in (22) - (26) works adequately faster than the learning rate of the auxiliary regressors in (29) and (30), i.e. $\kappa < \frac{1}{k_{FF}}$. Sliding Mode adaptation gain, ω_1 and ω_2 should be chosen large enough to overcome the inherent disturbance as analysed in (52). Increasing ω_2 in tandem with ω_1 will assist to drive the system to be more stable as analysed in (50). To guarantee finite-time convergence in the parameter estimates to its true values, ω_1 should be chosen as to satisfy (62c). The control gains, K_{r_1} and K_{r_2}, should be chosen large enough to effectively reject disturbance whilst satisfying (53).

Table 2: Adaptation Mechanism Parameters

Parameter Description	Symbols	Values
Parameter Estimation Adaptive weights, Γ (36)	γ_1	15
	γ_2	15
Forgetting Factor (29)(30)	k_{FF}	0.1
Filter Constant (22)-(26)	κ	0.02
Sliding Mode Adaptive weights, Ω (37)	ω_1	40
	ω_2	1
Control Gains, K_{r_i} (11)	K_{r_1}	10
	K_{r_2}	5
Sliding Mode Gain (8)(10)	λ	0.5
	Λ	$0.5I$

4.2. Algorithm Performance without disturbance, $T_d = 0$- Simulation Results

Figure 3 [21] shows the simulated result of the novel robust adaptive control in contrast to other two standard adaptive controls, i.e., gradient and least-square (LS) based adaptive control [27] with the case of no disturbance, $T_d = 0$. Excellent tracking performances for both elbow flexion and shoulder flexion are shown. $\hat{M}_1$ and $\hat{M}_2$ converge faster to the true value: 2.35 kg and

3 kg as compared to the two traditional algorithms (gradient and LS)(see Figure 3c and 3d). This is also confirmed in comparison to the standard gradient and LS based algorithm usually used in this context.

Convergence of parameter estimation errors denoted by $\tilde{\Theta}_1=(M_1 - \hat{M}_1)$ and $\tilde{\Theta}_2=(M_2 - \hat{M}_2)$ to zero can be verified through performance index computation, i.e., the mean Integral Absolute Error ($E_{I\bar{A}E_i}$) as shown in Table 3. The $E_{I\bar{A}E_i}$ can be computed by:

$$E_{I\bar{A}E_{i_{mass}}} = \frac{\sum_T \|M_{true_i} - \hat{M}_i\|}{T}, \qquad E_{I\bar{A}E_{i_{\tilde{q}}}} = \frac{\sum_T \|q_i(t) - q_{di}(t)\|}{T} \qquad (63)$$

where T is the length of time of the estimation, M_{true_i} is the actual value of the respective, i parameter, $\hat{M}_i$ is the parameter estimate, q_i is the joint angle of the controlled limb and q_{di} is the joint angle setpoint. The tracking performance of the proposed novel algorithm supersedes that of the gradient and LS based estimation approach. However, it is apparent to see that the estimation performance of the LS based algorithm is the worst although its tracking performance gains a greater benefit from the parameter estimation in comparison to the gradient algorithm: The LS based algorithm manages to track the given setpoint q_{di} well (better than the gradient) only after 30 seconds. Nevertheless, the significant performance contrast of our novel algorithm in comparison to these standard algorithms throughout simulation in terms of *robustness* and *convergence* confirms the theoretical discussion in Remark 2.
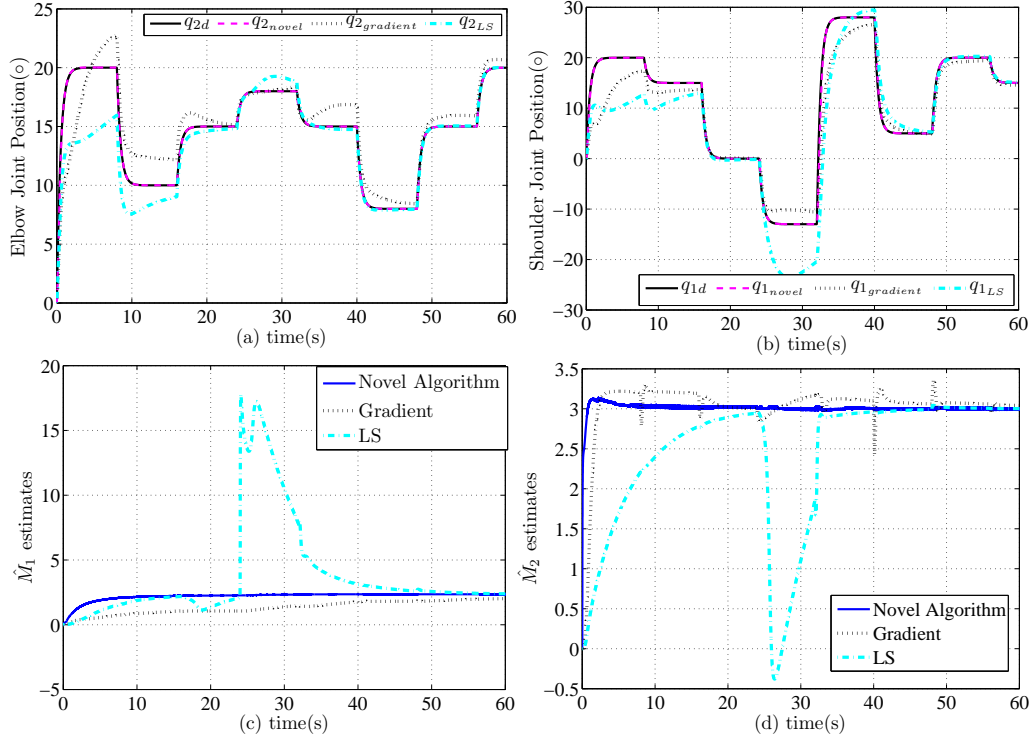
Figure 3: Novel Adaptive Control of manipulator in the case of no disturbance, $T_d = 0$

Table 3: $E_{I\bar{A}E_i}$ for the case of without disturbance, $Td = 0$

Associated Performance Parameters	$E_{I\bar{A}E_{i_{mass/\tilde{q}}}}$		
	Novel algorithm	Gradient	Least-Square
$\tilde{M}_1$	0.1262	0.7178	2.0889
$\tilde{M}_2$	0.0132	0.1270	0.5800
$\tilde{q}_1$	0.0021	0.0417	0.0680
$\tilde{q}_2$	4.7175e-004	0.0231	0.0205

Table 3 shows the tracking and parameter estimation performance measured by the given performance index in (63).

4.3. Algorithm Performance with bounded disturbance, T_d-Simulation Results

In contrast to [21], an additive bounded disturbance, T_d, is introduced in the robotic arm system. T_d comprises of a Band-Limited White noise with magnitude power of 0.1 and a sampling time $t_s = 0.02$ sec. The inherent robustness property (both in the tracking performance as well as in the parameter estimation) of the proposed algorithm is apparent in contrast to the gradient-based and LS-based algorithm as seen in Figure 4. It is interesting to see that the estimation by the LS-based algorithm is quite sensitive to changes in joint angle of more than $\pm 15°$ during the transient convergence (between 0 to 10 seconds) of its Γ matrix (see Remark 2 for LS algorithm's structure) as evident in Figure 4. One of the design parameter in LS-based algorithm β govern the speed of the parameter convergence. A compromise should be made between robustness and fast convergence. Figure 4a and Figure 4b show that the tracking performance of both the elbow and shoulder flexion motion for the novel adaptation algorithm are excellent despite of the presence of disturbance. The command signal for the shoulder and elbow flexion is,

$$q_{1_d} = 20 + \sin(0.1t + 2) + 16\sin(0.2t + 10) + 18\sin(0.3t + 12) \qquad (64a)$$

$$q_{2_d} = 24 + 8\sin(0.2t + 2) + 6\sin(0.3t + 10) + 9\sin(0.36t + 12) \qquad (64b)$$

The command signal is specially chosen as to satisfy the Sufficient Richness (SR) condition. The parameter estimation performance of the proposed algorithm (in contrast to the gradient and LS based) is evidently very good, exemplifying its ability to reject disturbance as seen in Figure 4c and 4d. For the novel algorithm, the estimate for $\hat{M}_1$ converges in less than 20 seconds whilst for $\hat{M}_2$, it achieves in a mere 3 seconds. By contrast, the gradient based algorithm's estimate for $\hat{M}_1$ converges at a much slower rate. The estimate of $\hat{M}_2$ by the LS-based algorithm shows a significant susceptibility to the disturbance. Referring to Table 4, the novel algorithm estimation performance (for the estimates $\hat{M}_1$ and $\hat{M}_2$) achieves the mean IAE values ($E_{I\bar{A}E}$) of 0.1457 and 0.0292 which are far better than that for the gradient based algorithm which has the mean IAE of 0.6120 and 0.2394. With the case of the LS-based algorithm, the mean IAE for estimating M_1 and M_2 is 0.4844 and 0.4290 respectively. Although the LS-based algorithm achieves a better estimation performance in comparison to the gradient-based approach for the mass estimation of the forearm mass $\hat{M}_1$, it suffers greatly when estimating the mass of the upperarm $\hat{M}_2$, judged by its corresponding $E_{I\bar{A}E}$ in Table 4.

The heavy reliance on the PE condition by the LS-based algorithm is evident here as its $E_{I\bar{A}E}$ scores better in this simulation with the given SR-satisfied command signal (64a)(64b) than its previous simulation without SR signal and disturbance (Compare Table 3 and Table 4).
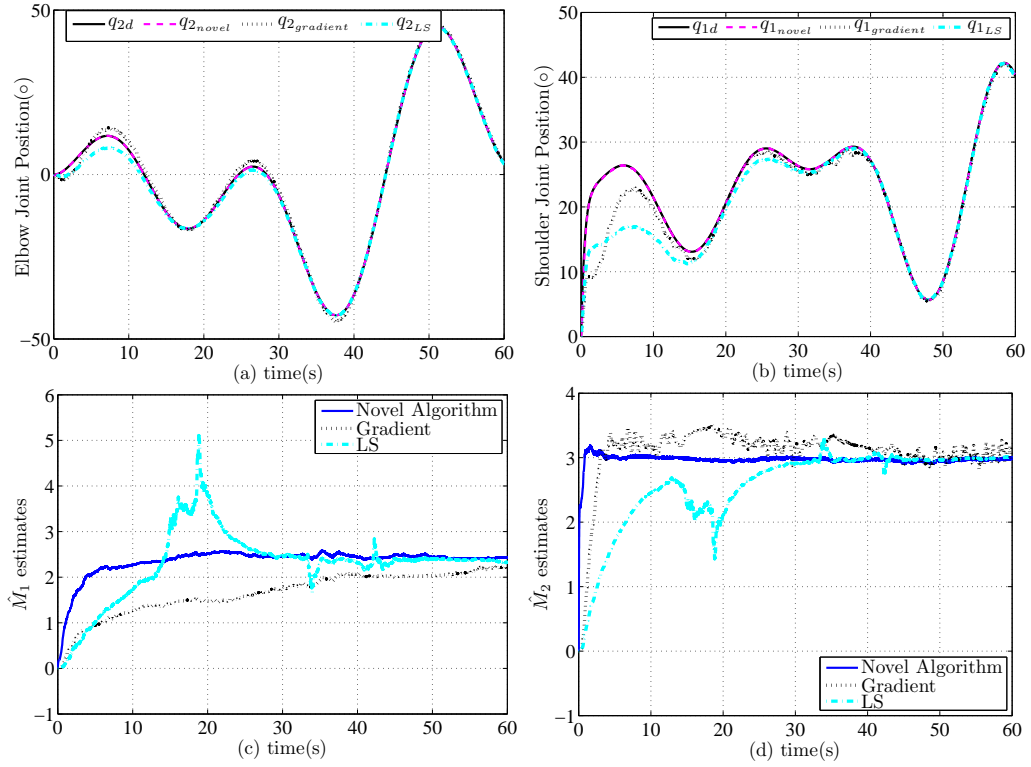

Figure 4: Tracking and Estimation performance of Novel Adaptive Control of manipulator(solid line for estimation) in contrast to Gradient-based approach(dashed line for estimation) and LS-based approach(dash-dotted line for estimation) in the case of additive bounded disturbance, T_d with command signal in (64a)(64b)

Table 4: $E_{I\bar{A}E_i}$ for the case of SR demand signal with disturbance

Associated Performance Parameters	$E_{I\bar{A}E_{i_{mass/\tilde{q}}}}$		
	Novel algorithm	Gradient	Least-Square
$\tilde{M}_1$	0.1457	0.6120	0.4844
$\tilde{M}_2$	0.0292	0.2394	0.4290
$\tilde{q}_1$	9.2315e-004	0.0271	0.0378
$\tilde{q}_2$	5.2279e-004	0.0185	0.0150
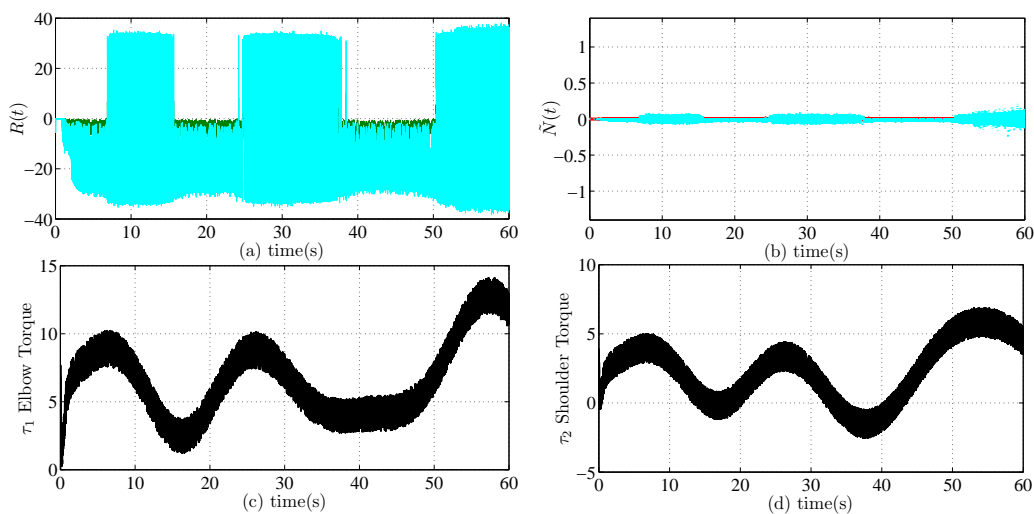
Figure 5: (a) The adaptive term $R(t)$ vector, (b) The bounded estimation error, $\tilde{N}(t)$ and the respective joint torque of (c) elbow and (d) shoulder in the case of disturbance, T_d

Referring to Figure 5b, $\tilde{N}(t)$ constitutes the parameter estimation error implicitly defined in the proposed algorithm. Clearly, $\tilde{N}(t)$ remains bounded close to zero, while the initial value is at magnitudes well above 1. The torque applied to both the BLDC motor at elbow and shoulder flexion are bounded (Figure 5c and Figure 5d).

The algorithm is also examined by introducing demands in the form of successive second order filtered steps in the presence of additive disturbance as shown in Figure 6. The tracking performance of the proposed algorithm (see Figure 6a, 6b) remains excellent whilst, the gradient-based algorithm tracking performance deteriorates. For both joints, elbow flexion and shoul-

22

der flexion, the proposed algorithm tracks the setpoint without compromising the performance of the mass estimations. The mass estimation by the proposed algorithm as presented in Figure 6c, 6d is acceptable. This contrasts to the gradient and LS-based algorithm, for which the estimated values tend to drift away. This can be accurately measured by the performance index, $E_{I\bar{A}E}$, in Table 5 where the novel algorithm exhibits an acceptable robustness in the presence of disturbance whilst the integrity of the tracking performance is not compromised. Figure 7b shows that the estimation error $\tilde{N}(t)$ remains bounded within 0.1% of the magnitude of the introduced filtered disturbance T_{dN} (33) and subsequent step changes in the setpoint. Figure 7a shows the bounded adaptive term $R(t)$, responsible in computing the parameter estimation error, effectively reacts against disturbance. Figure 7c and 7d show that the elbow and shoulder torque are bounded throughout the trajectories.
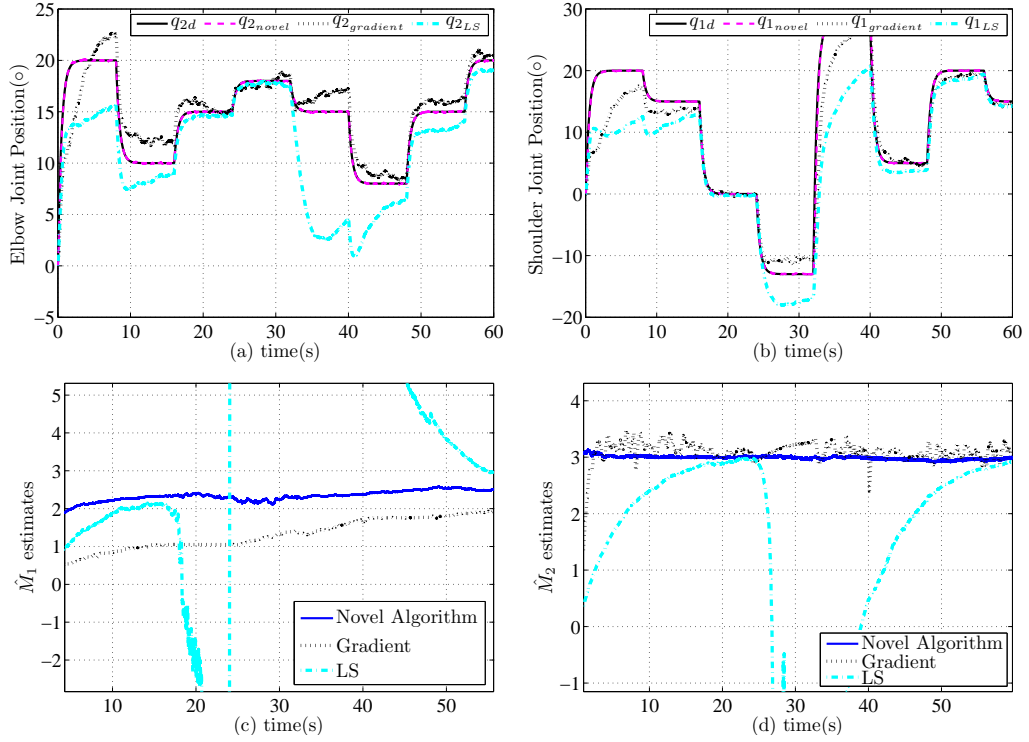
Figure 6: Tracking and Estimation performance of Novel Adaptive Control of manipulator (solid line for estimation) in contrast to Gradient-based approach (dashed line for estimation) and LS-based approach(dash-dotted line for estimation) in the case of additive bounded disturbance, T_d with successive filtered steps demand

Table 5: $E_{I\bar{A}E_i}$ for the case of successive filtered steps demand with disturbance

Associated Performance Parameters	$E_{I\bar{A}E_{i_{mass/\tilde{q}}}}$		
	Novel algorithm	Gradient	Least-Square
$\tilde{M}_1$	0.1417	0.9398	6.1916
$\tilde{M}_2$	0.0188	0.1674	2.4887
$\tilde{q}_1$	0.0025	0.0412	0.0771
$\tilde{q}_2$	8.6191e-004	0.0242	0.0563

24
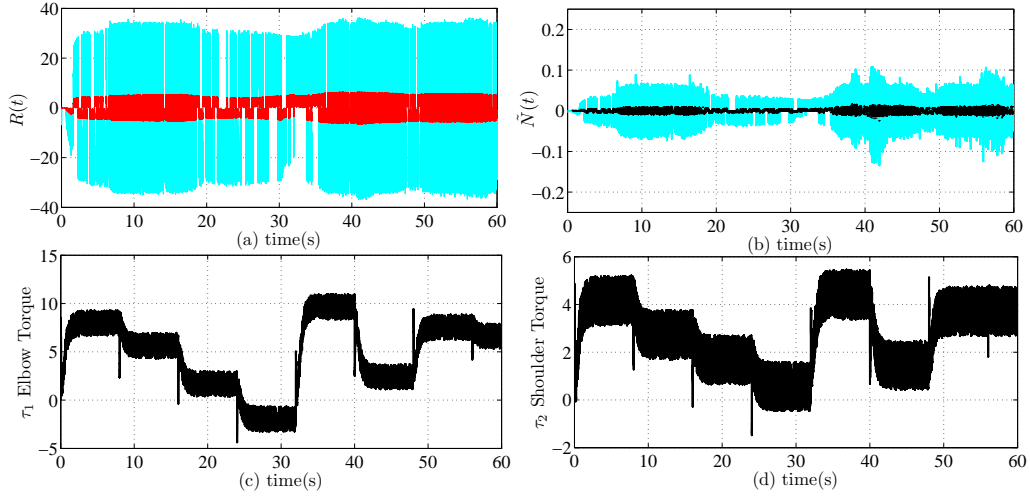
Figure 7: (a) The adaptive term $R(t)$, (b) The bounded estimation error, $\tilde{N}(t)$ and the respective joint torque of (c) elbow and (d) shoulder in the case of disturbance, T_d

To observe whether the system is persistently excited, the condition number of the auxiliary regressor, $W(t)$ is computed by taking $\|W(t)\|\|W^{-1}(t)\|$ (see Figure 8). The condition number of $W(t)$ remains mainly below 200, which shows sufficient levels of persistent excitation for $W(t)$, as $W(t)$ is clearly nonsingular. Figure 8 also shows that having a sufficiently rich command signal will assist in the parameter estimation performance by consequently keeping the condition number small at values below 150. Referring to the simulation results, it is evident that out of the three compared algorithms, the LS-based algorithm is the worst in terms of tracking and estimation. Therefore, we practically test the performance of the two best algorithms. Thus, relevant results are presented in the next section.
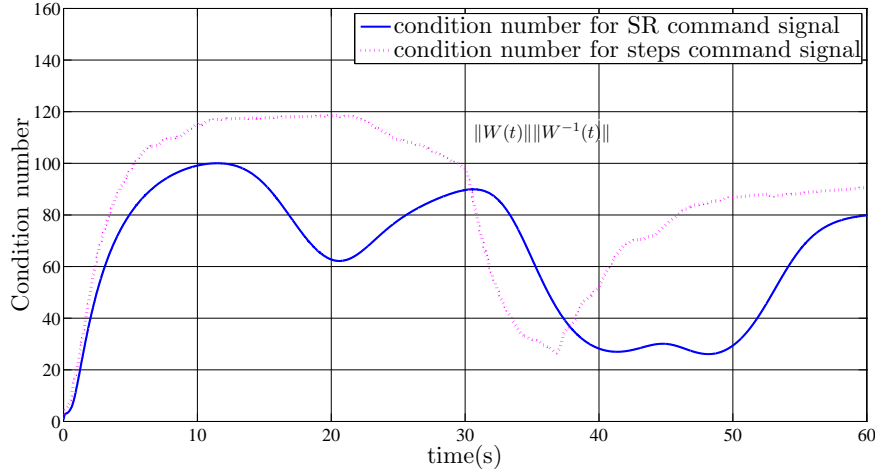
Figure 8: The condition number, $\|W(t)\|\|W^{-1}(t)\|$, of the auxiliary regressor

4.4. Practical Implementation

Figure 9a shows the implementation results of the applied novel adaptive control algorithm on BERT II humanoid system in comparison to the gradient based approach (Figure 9b). A sinusoidal command signal is given as the reference signal. Tracking performance for joint elbow flexion is comparable between the novel adaptive control algorithm and gradient-based approach. The $E_{I\bar{A}E}$ computed for elbow tracking shows that the novel algorithm is slightly better,i.e. its respective $E_{I\bar{A}E}$ is 2.0066 in comparison to the gradient-based approach which is 2.1547. In addition, the link mass estimation of BERT II robot arm in Figure 11a hovers around acceptable bounded values considering the fact that the proposed algorithm's regressor is formulated under the assumption that the robot arm has a uniform cylindrical shape (which they are not in the real case). The mass estimation as with the case of gradient based approach settles at incorrect values below zero as shown in Figure 11b. Figure 10a,b shows a bounded $\tilde{N}(t)$ with the adaptive term $R(t)$ in Figure 10c,d of the novel algorithm. As with the case of successive step demands, Figure 12 reveals excellent tracking performance for both joints, elbow and shoulder flexion. The compensation from the fast finite-time parameter estimation algorithm is advantageous to the control effort. The corresponding applied torque on the BLDC motor at both joints show that the control signal is bounded and of acceptable value.
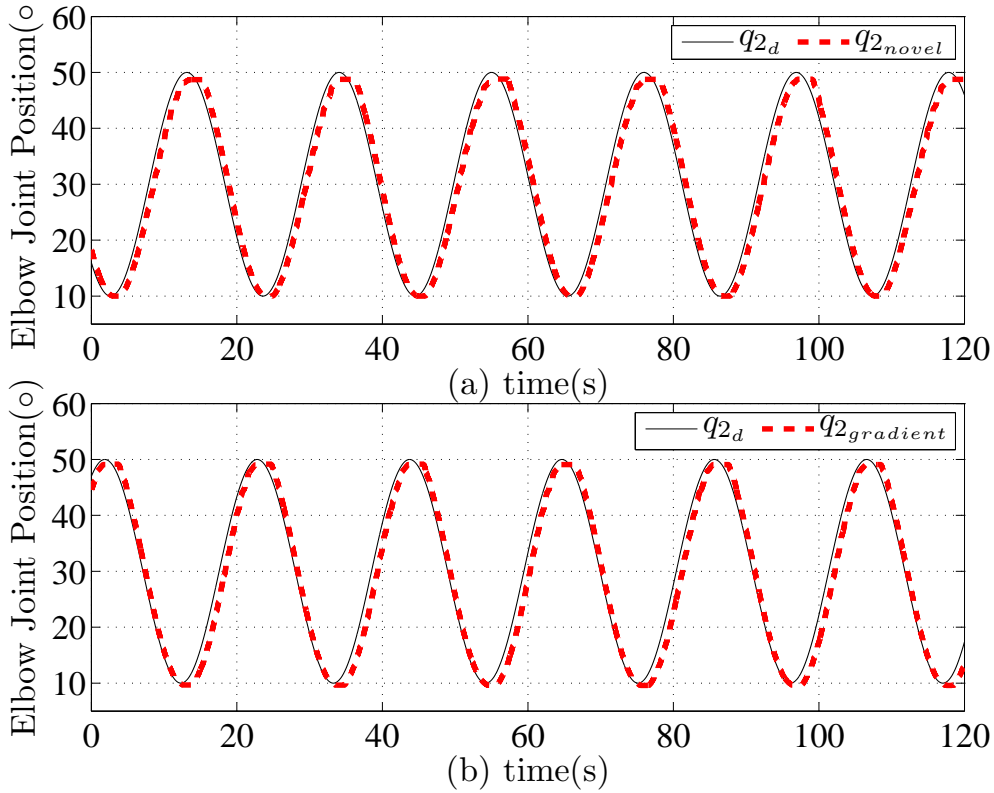
26

Figure 9: The tracking performance of the applied novel adaptive control for elbow (a) flexion of BERT II in comparison to the gradient-based approach (b).

5. Conclusion

A novel robust adaptive control algorithm featuring finite-time parameter estimation for humanoid robot arm is presented. The sliding-mode feature introduced both in the tracking and estimation scheme provides two-fold benefits. One is to provide significant levels of robustness against bounded disturbance both within the tracking error and estimation error. The second benefit is that finite-time convergence in the parameter estimation error can be guaranteed given sufficient PE or SR condition in the regressors. The reconstruction of a special auxiliary matrix is shown here by the use of an auxiliary filtered regression vector and filtered computed torque in the adaptive algorithm. This is instrumental to the machinery of the algorithm, from which then the sliding term can be incorporated in the adaptive law, allowing the unknown parameters, i.e. M_1 and M_2, to be estimated in finite-time.
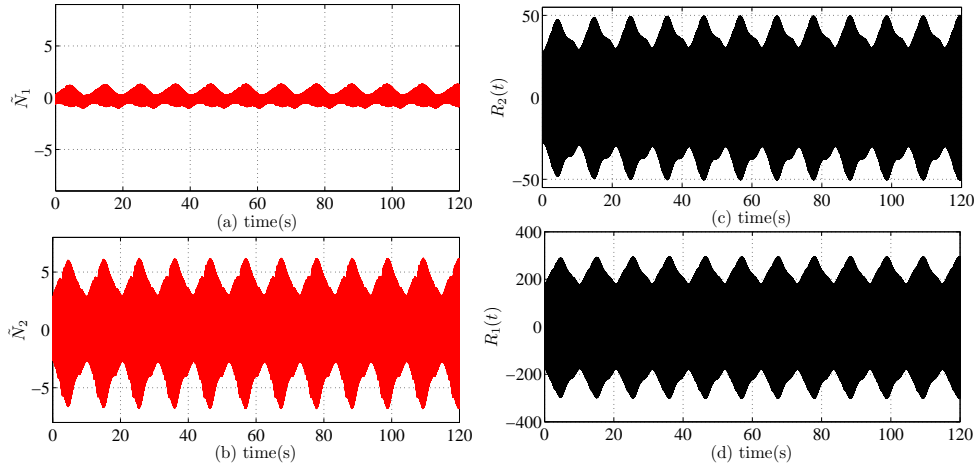
Figure 10: The bounded estimation error, $\tilde{N}(t)$ and the adaptive term, $R(t)$

As a direct consequence, parameter error convergence to zero can then be guaranteed with the PE or SR condition fulfilled. Robustness of the algorithm is also evident in the theoretical formulation by the subsumed leakage term in the adaptive law. Finite-time convergence in parameter estimation error is proven through a theoretical framework, simulation and practical implementation on a BERT II humanoid arm system. Practical methods using a condition number analysis to verify persistent excitation are suggested. The experimental results show that the adaptive scheme improves tracking performance.
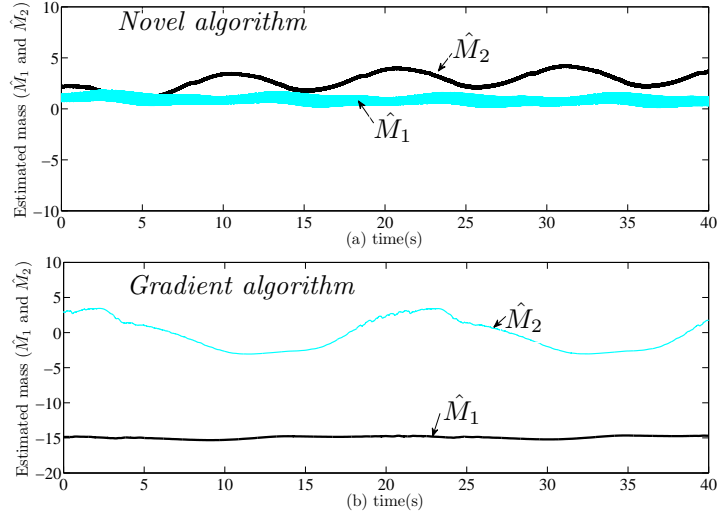
6. Acknowledgments

28

Figure 11: The link mass estimation performance of the novel algorithm (a) in comparison to the gradient-based approach (b).
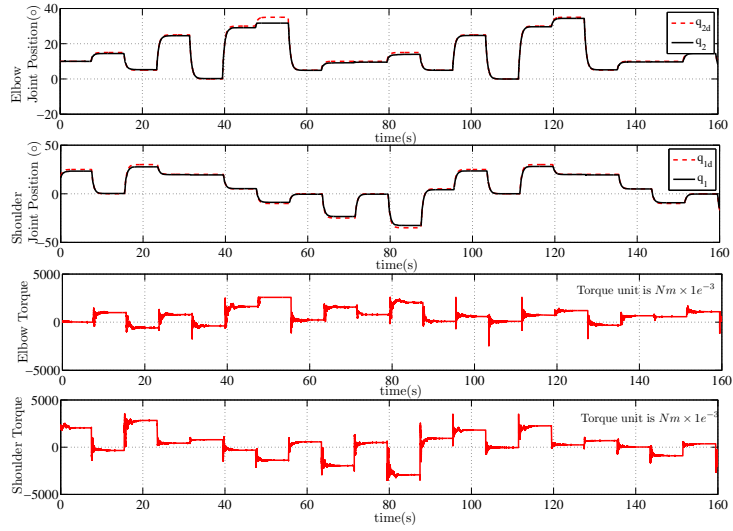

Figure 12: The tracking performance of the applied novel adaptive control for shoulder and elbow flexion joint of BERT II with its corresponding applied torque

29

References

[1] M. W. Spong, M. Vidyasagar, Robot Dynamics and Control, Wiley, 1989.

[2] J.-J. Slotine, W. Li, Composite adaptive control of robot manipulators, Automatica 25 (1989) 509–519.

[3] J.-J. Slotine, Adaptive manipulator control: A case study, IEEE Transactions on Automatic Control 33 (11) (1988) 995–1003. doi:10.1109/9.14411.
URL http://ieeexplore.ieee.org/lpdocs/epic03/wrapper.htm?arnumber=14411

[4] R. Horowitz, M. Tomizuka, An adaptive control scheme for mechanical manipulators- compensation of nonlinearity and decoupling control, ASME Winter Annual meeting.

[5] T. C. Hsia, Adaptive control of robotic manipulators-a review, in: IEEE Int. Conf. on Robot and Automation, 1986.

[6] K. Lim, M. Eslami, Robust adaptive controller design for robot manipulators systems, IEEE Journal of Robotics and Automation 3 (1987) 54–66.

[7] C. Lee, M. J. Chung, An adaptive trajectory control of manipulators, IEEE Transaction of Automatic Control AC-29 (1984) 837–840.

[8] A. Koivo, T. Guo, Adaptive linear controller for robotic manipulators, IEEE Transaction of Automatic Control AC-28 (1983) 162–171.

[9] M. Vukobratovic, N. Kircanski, An approach to adaptive control of robotic manipulators, Automatica 21 (1985) 639–647.

[10] R. Ortega, M. W. Spong, Adaptive motion control of rigid robots: a tutorial, Automatica 25 (1989) 877–888.

[11] J.-J. Slotine, W. Li, Adaptive robot control. a case study, in: IEEE Int. Conf. on Robotics and Automation, Raleigh, North Carolina, 1987.

[12] J.-J. Slotine, W. Li, Adaptive strategies in constrained manipulation, in: IEEE Int. Conf. on Robotics and Automation, Raleigh, North Carolina, 1987.

[13] J. Craig, H. P., S. Sastry, Adaptive control of mechanical manipulators, in: IEEE Int. Conf. on Robotics and Automation, San Francisco, California, 1986.

[14] W. Li, J.-J. Slotine, An indirect adaptive robot controller, Systems & Control Letters 12 (1989) 259–266.

[15] P. Hsu, S. Sastry, M. Bodson, B. Paden, Adaptive identification and control of manipulators without joint acceleration measurements, in: IEEE Int. Conf. on Robotics and Automation, 1987.

[16] F. L. Lewis, D. M. Dawson, C. T. Abdallah, Robot Manipulator Control; Theory and Practice, 2nd Edition, Marcel Dekker, 2004.

[17] S. Khan, Adaptive and reinforcement learning control methods for active compliance control of a humanoid robot arm, Ph.D. thesis, University of the West of England (2012).

[18] J. Na, G. Herrmann, X. Ren, M. Mahyuddin, P. Barber, Robust adaptive finite-time parameter estimation and control of nonlinear systems, in: Intelligent Control (ISIC), 2011 IEEE International Symposium on, 2011, pp. 1014 –1019. doi:10.1109/ISIC.2011.6045402.

[19] V. Adetola, M. Guay, Finite-time Parameter Estimation in Adaptive Control of Nonlinear Systems, New York (2007) 1920–1924.

[20] M. N. Mahyuddin, J. Na, G. Herrmann, X. Ren, P. Barber, An adaptive observer-based parameter estimation algorithm with application to road gradient and vehicle's mass estimation, in: Control (CONTROL), 2012 UKACC International Conference on, 2012, pp. 102 –107. doi:10.1109/CONTROL.2012.6334614.

[21] M. N. Mahyuddin, G. Herrmann, S. Khan, A novel adaptive control algorithm in application to a humanoid robot arm, in: G. Herrmann, M. Studley, M. Pearson, A. Conn, C. Melhuish, M. Witkowski, J.-H. Kim, P. Vadakkepat (Eds.), Advances in Autonomous Robotics, Vol.

7429 of Lecture Notes in Computer Science, Springer Berlin / Heidelberg, 2012, pp. 25–36.

[22] J. Reed, P. Ioannou, Instability analysis and robust adaptive control of robotic manipulators, IEEE Transaction of Robotics and Automation RA-3 (1989) 381–386.

[23] Y. Li, S. S. Ge, C. Yang, Learning impedance control for physical robot–environment interaction, International Journal of Control 85 (2) (2012) 182–193.

[24] W. E. Dixon, I. D. Walker, D. M. Dawson, J. P. Hartranft, Fault detection for robot manipulators with parametric uncertainty: a prediction-error-based approach, Robotics and Automation, IEEE Transactions on 16 (6) (2000) 689–699.

[25] S. Sastry, M. Bodson, Adaptive control: Stability, Convergence and Robustness, Dover Publications, 1989.

[26] J.-J. Slotine, W. Li, Applied Nonlinear Control, Prentice Hall, 1990.
URL http://www.worldcat.org/isbn/0130408905

[27] P. Ioannou, J. Sun, Robust Adaptive Control, 1st Edition, Prentice Hall, 1996.

[28] G. Feng, A new adaptive control algorithm for robot manipulators in task space, IEEE Transactions on Robotics and Automation 11 (3) (1995) 457–462.

[29] C. Edwards, S. Spurgeon, Sliding mode control: theory and applications, CRC, 1998.

[30] S. Sastry, M. Bodson, Adaptive Control: Stability, Convergence and Robustness, Dover Books on Electrical Engineering Series, Dover, 2011.
URL http://books.google.co.uk/books?id=-cOviBa9pR8C

[31] M. Krstić, I. Kanellakopoulos, P. Kokotović, Nonlinear and adaptive control design, Adaptive and learning systems for signal processing, communications, and control, Wiley, 1995.
URL http://books.google.co.uk/books?id=wxkoAQAAMAAJ